Thulium pumped mid-infrared 0.9–9μm supercontinuum generation in concatenated fluoride and chalcogenide glass fibers

Kubat, Irnis; Petersen, Christian Rosenberg; Møller, Uffe Visbech; Seddon, Angela; Benson, Trevor; Brilland, Laurent; Méchin, David; Moselund, Peter M.; Bang, Ole

Published in:
Optics Express

Link to article, DOI:
10.1364/OE.22.003959

Publication date:
2014

Document Version
Publisher's PDF, also known as Version of record

Thulium pumped mid-infrared 0.9-9μm supercontinuum generation in concatenated fluoride and chalcogenide glass fibers

Irnis Kubat,[1] Christian Rosenberg Petersen,[1] Uffe Visbech Møller,[1] Angela Seddon,[2] Trevor Benson,[2] Laurent Brilland,[3] David Méchin,[3] Peter M. Moselund,[4] and Ole Bang[1,4]

[1] *DTU Fotonik, Department of Photonics Engineering, Technical University of Denmark, 2800 Kgs. Lyngby, Denmark*

[2] *George Green Institute for Electromagnetics Research, Faculty of Engineering, University Park, University of Nottingham, Nottingham NG7 2RD, UK*

[3] *Perfos, R&D Platform of Photonics Bretagne, 11 Rue Louis de Broglie, 22300 Lannion, France*

[4] *NKT Photonics A/S, Blokken 84, 3460 Birkerød, Denmark*

ikub@fotonik.dtu.dk

Abstract: We theoretically demonstrate a novel approach for generating Mid-InfraRed SuperContinuum (MIR SC) by using concatenated fluoride and chalcogenide glass fibers pumped with a standard pulsed Thulium (Tm) laser (T_{FWHM}=3.5ps, P_0=20kW, ν_R=30MHz, and P_{avg}=2W). The fluoride fiber SC is generated in 10m of ZBLAN spanning the 0.9-4.1μm SC at the -30dB level. The ZBLAN fiber SC is then coupled into 10cm of As_2Se_3 chalcogenide Microstructured Optical Fiber (MOF) designed to have a zero-dispersion wavelength (λ_{ZDW}) significantly below the 4.1μm InfraRed (IR) edge of the ZBLAN fiber SC, here 3.55μm. This allows the MIR solitons in the ZBLAN fiber SC to couple into anomalous dispersion in the chalcogenide fiber and further redshift out to the fiber loss edge at around 9μm. The final 0.9-9μm SC covers over 3 octaves in the MIR with around 15mW of power converted into the 6-9μm range.

OCIS codes: (060.2390) Fiber optics, infrared; (140.3070) Infrared and far-infrared lasers; (160.4330) Nonlinear optical materials; (160.2750) Glass and other amorphous materials.

References and links

1. S. Wartewig and R. H. H. Neubert, "Pharmaceutical applications of mid-IR and Raman spectroscopy," Adv. Drug Delivery Rev. **57**, 11441170 (2005).
2. A. Seddon, "Mid-Infrared (IR) - a hot topic: The potential for using mid-IR light for non-invasive early detection of skin cander in vivo," Phys. Status Solidi B **250**, 1020–1027 (2013).
3. R. Haus, K. Schäfer, W. Bautzer, J. Heland, H. Moseback, H. Bittner, and T. Eisenmann, "Mobile fourier-transform infrared spectroscopy monitoring of air pollution," Appl. Opt. **33**, 5682–5689 (1994).
4. A. Mukherjee, S. Von der Porten, and C. K. N. Patel, "Standoff detection of explosive substances at distances of up to 150 m," Appl. Opt. (2010).
5. M. Razeghi, S. Slivken, Y. Bai, and S. R. Darvish, "Quantum cascade laser: a versatile and powerfull tool," Opt. Photon. News **19**, 4247 (2008).
6. M. Pushkarsky, M. Weida, T. Day, D. Arnone, R. Pritchett, D. Caffey, and S. Crivello, "High-power tunable external cavity quantum cascade laser in the 5-11 micron regime," Proc. SPIE **6871**, 68711X–1 (2008).

#203541 - $15.00 USD Received 20 Dec 2013; revised 3 Feb 2014; accepted 3 Feb 2014; published 12 Feb 2014

7. J. M. Dudley, G. Genty, and S. Coen, "Supercontinuum generation in photonic crystal fiber," Rev. Mod. Phys. **78**, 1135–1184 (2006).
8. C. Xia, M. Kumar, M.-Y. Cheng, R. S. Hegde, M. N. Islam, A. Galvanauskas, H. G. Winful, and J. Fred L. Terry, "Power scalable mid-infrared supercontinuum generation in ZBLAN fluoride fibers with up to 1.3 watts time-averaged power," Opt. Express **15**, 865–871 (2007).
9. C. Xia, Z. Xu, M. N. Islam, J. Fred L. Terry, M. J. Freeman, and J. Mauricio, "10.5 W Time-averaged power mid-IR supercontinuum generation extending beyond 4 μm with direct pulse patteren modulation," IEEE J. Sel. Top. Quant. Electron. **15** (2009).
10. Q. Qin, X. Yan, C. Kito, M. Liao, C. Chaudhari, K. Suzuku, Y. Ohishi, "Supercontinuum generation spanning over three octaves from UV to 3.85μm in a fluoride fiber," Opt. Lett. **34** (2009).
11. P. M. Moselund, C. Petersen, S. Dupont, C. Agger, O. Bang, and S. R. Keiding, "Supercontinuum-broad as a lamp bright as a laser, now in the mid-infrared," Proc. **SPIE 8381**, 83811A (2012).
12. P. Moselund, C. Petersen, L. Leick, J. S. Dam, P. Tidemand-Lichtenberg, and C. Pedersen, "Highly stable, all-fiber, high power ZBLAN supercontinuum source reaching 4.75 µm used for nanosecond mid-IR spectroscopy," (2013), p. JTh5A.9.
13. R. Thapa, D. Rhonehouse, D. Nguyen, K. Wiersma, C. Smith, J. Zong, A. Chavez-Pirson, " Mid-IR supercontinuum generation in ultra-low loss, dispersion-zero shifted tellurite glass fiber with extended coverage beyond 4.5μm ," Proc. **SPIE 8898**, 889808-8 (2013).
14. NP Photonics Inc., "Tellurite based Mid-infrared Supercontinuum sources," Online at www.npphotonics.com (2013).
15. C. A. Michaels, T. Masiello, and P. M. Chu, "Fourier transform spectrometry with a near-infrared supercontinuum source," Appl. Spectrosc. **63**, 538543 (2009).
16. S. Dupont, C. Petersen, J. Thøgersen, C. Agger, O. Bang, and S. R. Keiding, "IR microscopy utilizing intense supercontinuum light source," Opt. Express **20**, 4887–4892 (2012).
17. J. Swiderski and M. Michalska, "Mid-infrared supercontinuum generation in a single-mode thulium-doped fiber amplifier," Laser Phys. Lett. **10**, 035105 (2013).
18. V. Shiryaev and M. Churbanov, "Trends and prospects for development of chalcogenide fibers for mid-infrared transmission," J. Non-Cryst. Solids **377**, 225 – 230 (2013).
19. R. E. Slusher, G. Lenz, J. Hodelin, J. Sanghera, L. B. Shaw, and I. D. Aggarwal, "Large Raman gain and nonlinear phase shift in high-purity As_2Se_3 chalcogenide fibers," J. Opt. Soc. Am. B **21**, 1146–1155 (2004).
20. J. Hu, and C. R. Menyuk, L. B. Shaw, J. S. Sanghera, and I. D. Aggarwal, "Maximizing the bandwidth of supercontinuum generation in As_22Se_3 chalcogenide fibers," Opt. Express **18**, 6722–6739 (2010).
21. R. R. Gattass, L. B. Shaw, V. Q. Nguyena, P. C. Purezaa, I. D. Aggarwal, J. S. Sangheraa, "All-fiber chalcogenide-based mid-infrared supercontinuum source," Opt. Fib. Technol. **18** (2012).
22. W. Yuan, "2-10 μm mid-infrared supercontinuum generation in As_2Se_3 photonics crystal fiber," Laser Phys. Lett. **10**, 095107 (2013).
23. C. Wei, X. Zhu, R. A. Norwood, F. Song, and N. Peyghambarian, "Numerical investigation on high power mid-infrared supercontinuum fiber lasers pumped at 3 μm," Opt. Express **21**, 29488–29504 (2013).
24. M. Bache, H. Guo, and B. Zhou, "Generating mid-IR octave-spanning supercontinua and few-cycle pulses with solitons in phase-mismatched quadratic nonlinear crystals," Opt. Express **3**, 1647–1657 (2013).
25. Y. Yu, X. Gai, T. Wang, P. Ma, R. Wang, D.-Y. C. Z. Yang, S. Madden, and B. Luther-Davies, "Mid-infrared supercontinuum generation in chalcogenides," Opt. Mat. Express **3**, 1075–1086 (2013).
26. P. Ma, D.-Y. Choi, Y. Yu, X. Gai, Z. Yang, S. Debbarma, S. Madden, and B. Luther-Davies, "Low-loss chalcogenide waveguides for chemical sensing in the mid-infrared," Opt. Express **21**, 29927–29937 (2013).
27. C. Agger, S. T. Sørensen, C. L. Thomsen, S. R. Keiding, and O. Bang, "Nonlinear soliton matching between optical fibers," Opt. Lett. **36**, 2596–2598 (2011).
28. C. Hagen, J. Walewski, and S. Sanders, "Generation of a continuum extending to the midinfrared by pumping ZBLAN fiber with an ultrafast 1550-nm source," IEEE Photon. Technol. Lett. **18**, 91–93 (2006).
29. O.P. Kulkarni, V.V. Alexander, M. Kumar, M.J. Freeman, M.N. Islam, F.L. Terry, Jr., M. Neelakandan, and A. Chan, "Supercontinuum generation from 1.9 to 4.5m in ZBLAN fiber with high average power generation beyond 3.8m using a thulium-doped fiber amplifier," J. Opt. Soc. Am. B 28, 2486-2498 (2011).
30. J. Geng, Q. Wang, and S. Jiang, "High-spectral-flatness mid-infrared supercontinuum generated from a Tm-doped fiber amplifier," Appl. Opt. **51**, 834840 (2012).
31. AdValue Photonics Fiber Lasers , "Two-micron thulium-doped fiber lasers achieve 10 kW peak power (feature article in Laser Focus World Feb. 2013 issue)," Online at http://www.advaluephotonics.com/ (2013).
32. F. Gan, "Optical properties of fluoride glasses: a review," Journal of non-crystalline solids **184**, 9–20 (1995).
33. FiberLabs Inc., "Fluoride fibers," Online at http://www.fiberlabs-inc.com/ (2013).
34. Amorphous, Materials Inc., "Amtir-2," Online at http://www.amorphousmaterials.com/ (2013).
35. L. Brilland and D. Méchin, "Loss measurements of a 20μm As_2Se_3 grapefruit fiber," Private communication, 2013.
36. D. Marcuse, "Loss analysis of single-mode fiber splices," Bell Syst. Tech. J. **56**, 703–718 (1977).
37. I. Kubat, C. S. Agger, P. M. Moselund, and O. Bang, "Mid-infrared supercontinuum generation to 4.5um in

#203541 - $15.00 USD Received 20 Dec 2013; revised 3 Feb 2014; accepted 3 Feb 2014; published 12 Feb 2014

uniform and tapered ZBLAN step-index fibers by direct pumping at 1064 and 1550nm," J. Opt. Soc. Am. B **30**, 2743–2757 (2013).
38. J. Troles, Q. Coulombier, G. Canat, M. Duhant, W. Renard, P. Toupin, L. Calvez, F. S. G. Renversez, M. E. Amraoui, J. L. Adam, T. Chartier, D. Méchin, and L. Brilland, "Low loss microstructured chalcogenide fibers for large non linear effects at 1995nm," Opt. Express **18**, 26647–26654 (2010).
39. J.-L. Adam, J. Trolès, and L. Brilland, "Low-loss mid-ir microstructured optical fibers," in "Optical Fiber Communication Conference," (2012), p. OM3D.2.
40. J. H. Price, X. Feng, A. M. Heidt, G. Brambilla, P. Horak, F. Poletti, G. Ponzo, P. Petropoulos, M. Petrovich, J. Shi, M. Ibsen, W. H. Loh, H. N. Rutt, and D. J. Richardson, "Supercontinuum generation in non-silica fibers," Opt. Fiber. Technol. **18**, 327 – 344 (2012).
41. M. D. Nielsen, G. Vienne, and J. R. Folkenberg, "Investigation of microdeformation-induced attenuation spectra in a photonic crystal fiber," Opt. Lett. **28**, 236–238 (2003).
42. N. A. Mortensen and J. R. Folkenberg, "Low-loss criterion and effective area considerations for photonic crystal fibers," J. Opt. A: Pure Appl. Opt. **5**, 163–167 (2003).
43. P. J. Roberts, F. Couny, H. Sabert, B. J. Mangan, T. A. Birks, J. C. Knight, and P. St. J. Russell, "Loss in solid-core photonic crystal fibers due to interface roughness scattering," Opt. Express **28**, 236–238 (2005).
44. B. Ung and M. Skorobogatiy, "Chalcogenide microporous fibers for linear and nonlinear applications in the mid-infrared," Opt. Express **18**, 8647–8659 (2010).
45. C. Agger, C. Petersen, S. Dupont, H. Steffensen, J. K. Lyngsø, C. L. Thomsen, J. Thøgersen, S. R. Keiding, and O. Bang, "Supercontinuum generation in ZBLAN fibers - detailed comparison between measurement and simulation," J. Opt. Soc. Am. B **29**, 635–645 (2012).
46. M. Saad, "Heavy metal fluoride glass fibers and their applications," Proc. SPIE **8307**, 83070N–83070N–16.
47. J. Sanghera and I. Aggarwal, "Active and passive chalcogenide glass optical fibers for IR applications: a review," Journal of Non-Crystalline Solids **256-257**, 6 – 16 (1999).

1. Introduction

The Mid-InfraRed (MIR) part of the spectrum is a very exciting frequency region as absorption bands of many organic compounds reside herein, such as sugars, lipids, and proteins, which can be probed to differentiate malignant from benign tissue in detection of skin cancer [1, 2]. Absorption bands of atmospheric molecules, such as CO_2 and NO_x, likewise reside within this part of the spectrum, as well as explosive materials such as TNT, which also can be probed for detection of air pollution [3] or in stand-off ranged detection of hazardous materials [4], respectively.

Traditionally, Fourier Transform InfraRed (FTIR) spectrometers are used to obtain transmission or reflection spectra of samples with weak globar type sources (emitting in the 1-20μm range). With the advent of Quantum Cascade Lasers (QCLs) spectroscopy has improved as the traditional broadband light sources like the globar in the FTIR could be replaced with a spatially coherent laser source yielding a high power density [5]. While tunable MIR QCLs operating at several wavelengths have been developed [6], a single QCL is still a laser operating at a narrow spectral range, so in order to have the spectral range offered by the globar, multiple expensive QCLs operating at different wavelengths need to be combined together. Supercontinuum sources combine all features of a broadband and spatially coherent source having a high intensity [7]. Mid-IR SC laser sources are currently based primarily on ZBLAN fibers covering the 1-4.75μm spectral range [8-12] and tellurite fibers covering the 1-5μm range [13, 14]. Mid-IR SC sources have already been successfully applied in FTIR spectroscopy [15] and in hyperspectral imaging [16]. A further advantage of fiber based laser sources is that the average power can be scaled up by increasing the pump power [9, 17], or by increasing the pump repetition rate [8, 9], with the current record being a 10.5W average power ZBLAN SC demonstrated by Xia et al. [9].

In order to extend the SC spectrum further into the MIR region, materials other than fluoride and tellurite are needed. For this the chalcogenide glasses (CHALCs) are good candidates as some compositions have been shown to be able to transmit light out to 25μm [18]. Apart from the broadband MIR transmission windows, CHALCs posses very large linear and nonlinear

#203541 - $15.00 USD Received 20 Dec 2013; revised 3 Feb 2014; accepted 3 Feb 2014; published 12 Feb 2014

refractive indices as shown by Slusher *et al.* [19]. These two features combined have resulted in an intensified research of developing MIR SC sources based on CHALC waveguides and fibers; Hu *et al.* show theoretically that it is possible to obtain a 2-7μm MIR SC in optimised As-Se MOFs when pumping at 2.5μm with 1kW pulses [20]. Gattas *et al.* show experimentally that a 1.9-4.8μm MIR SC is obtainable when pumping As-S fibers with Tm amplified picosecond pulses coming from an Er source [21]. Yuan has numerically shown how formation of SC in a As_2Se_3 Microstructure Optical Fiber (MOF), having an idealised loss without extrinsic impurities, otherwise typically present in a fabricated fiber, can give a 2-10μm output when pumped with femtosecond pulses having 10kW peak power at 4.1μm [22]. Wei *et al.* likewise numerically obtained a broadband 2-12μm SC in As_2Se_3 MOF, but in this case pumping at 2.78μm with 1kW peak power femtosecond pulses from a mode-locked Er:ZBLAN laser [23]. In a low loss $LiInS_2$ planar waveguide Bache *et al.* showed numerically that it is possible to obtain a 1-8μm SC in just 15mm of waveguide when pumping with femtosecond pulses having a peak power of 120MW launched at 3μm from a tunable Optical Parametric Amplifier (OPA) [24]. Experimentally Yu *et al.* used an OPA generating femtosecond pulses having 20MW peak power at 5.3μm, where they were able to demonstrate a 2.5-7.5μm SC by pumping a bulk $Ge_{11.5}As_{24}Se_{64.5}$ sample [25]. Waveguides of the same glass composition have also been successfully utilised in MIR chemical sensing [26].

In some of the pump lasers used the peak power is *very high* of several megawatts and coming from a tunable laser source such as in [24, 25]. While these are good approaches for a first theoretical and experimental realisation of a CHALC MIR SC source, such lasers are impractical to introduce in commercial SC products without making them complex and very expensive. The MIR SC designs using a single wavelength pump laser with peak power around 1-10kW, such as 2.5μm in [20], 2.78μm in [23], and 4.1μm in [22], are potentially more commercially feasible. However, these laser sources are not yet commercially available, and thus the proposed SC sources are currently only of academic interest, such as in particular the 4.1μm pump proposed to be generated by down-converting a thulium laser [22].

We circumvent these two issues by approaching the generation of MIR SC by concatenating fluoride and CHALC fibers as this is an easier setup to implement in practice with all the required components being readily available, which makes it also a more commercially friendly approach. The SC concatenation approach relies on the fact that a typical SC spectrum is composed of many solitons in the long wavelength part of the spectrum with anomalous dispersion, pushing the light to longer wavelengths [7]. The solitons are usually femtosecond long pulses having high peak powers, so when concatenating fibers the solitons from the first fiber can continue to redshift in the second fiber, which allows the spectral broadening to proceed, provided the effective soliton number of each individual soliton in the second fiber is larger than 0.5 [27]. In our case the second fiber is a highly nonlinear CHALC fiber and so the transferred solitons will have soliton numbers significantly above 1.5 and therefore undergo soliton fission, which leads to extended redshift and spectral broadening [27].

Conceptually the SC concatenation approach was used before to generate a ZBLAN SC to about 4μm by using an erbium laser pumping a piece of silica fiber to generate a silica SC out to 2.2μm and then coupling this into a ZBLAN fiber [8, 9, 28]. Later this concatenated approach was improved by amplifying the silica SC using a section of core-pumped thulium amplifier, before coupling it into a ZBLAN [29, 11, 30] or a chalcogenide fiber [30]. Here we present the first demonstration of how the cascading approach, without intermediate amplifiers, can be used to generate an SC all the way to 9μm.

#203541 - $15.00 USD Received 20 Dec 2013; revised 3 Feb 2014; accepted 3 Feb 2014; published 12 Feb 2014

2. Concatenated fluoride and chalcogenide glass fiber supercontinuum generation

We extended the ZBLAN fluoride fiber MIR SC by concatenating it with a CHALC fiber that allowed the formation of SC to proceed further into the MIR part of the spectrum, as shown in Fig. 1(a).

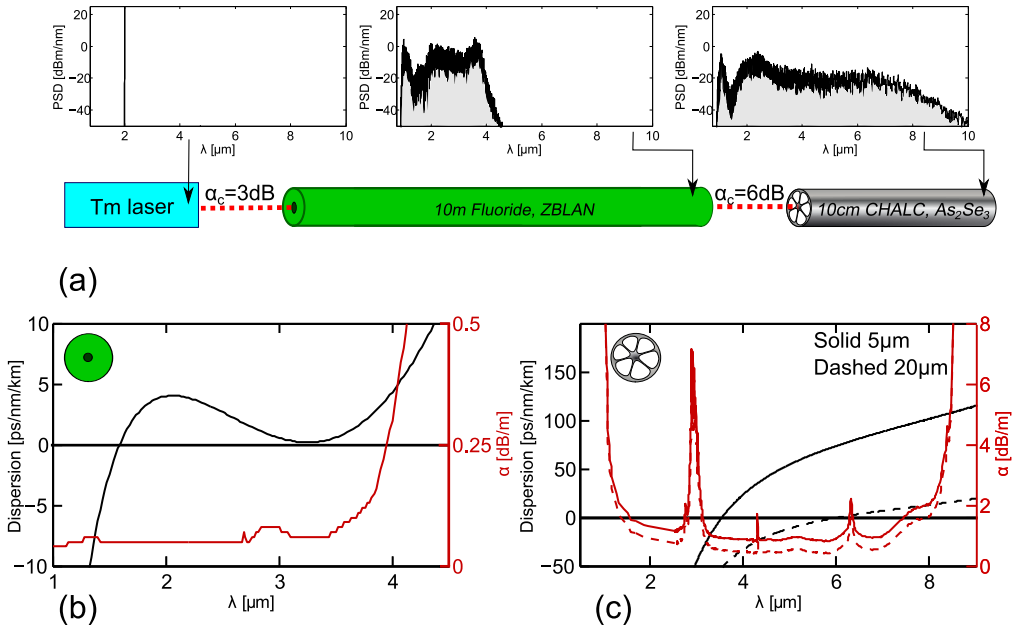

Fig. 1. Setup of the concatenated MIR SC source. (a) The Tm laser (T_{FWHM}=3.5ps, P_0=20kW, ν_r=30MHz, P_{avg}=2W) was coupled to a ZBLAN step-index fiber with a coupling loss of 3dB, where it generated a 0.9-4.1μm SC (-30dB level). The output SC was further coupled into a CHALC As_2Se_3 MOF with a coupling loss of 6dB, in which it generated a 0.9-9μm SC (-30dB level). The spectrum above shows how a single pulse undergoes spectral broadening through the setup. (b) Dispersion for a ZBLAN fiber with core diameter of 5.7μm and NA=0.30 based on material dispersion by F. Gan [32] and measured loss provided by FiberLabs Inc., Japan [33]. (c) Optical properties of the chalcogenide grapefruit MOF with core diameter of 5 (solid) and 20μm (dashed) based on As_2Se_3 material dispersion by Amorphous Materials Inc. [34] and loss for the fiber of the same material and design provided by Perfos [35].

A Tm fiber laser operating at 2μm emitting Gaussian shaped pulses having a temporal duration T_{FWHM}=3.5ps, peak power P_0=20kW, repetition rate ν_R=30MHz, and average power P_{avg}=2W [31] drives the entire SC formation process by pumping first the ZBLAN fluoride Step-Index Fiber (SIF). We assumed a coupling loss of α_c=3dB when coupling the laser beam into the Fundamental Mode (FM) of the ZBLAN SIF, which occurred due to mode mismatch and Fresnel reflection at the interface of the ZBLAN fiber (n=1.49 at 2μm), so effectively P_0=10kW drives the broadening process. The ZBLAN fluoride fiber SC is then transferred to an As_2Se_3 CHALC MOF. Due to the broad bandwidth of the first SC we assume a typical increased coupling loss of α_c=6dB due to a large frequency dependent mode mismatch between the two different fiber geometries [36] as well as an enhanced Fresnel reflection at the CHALC fiber interface (n=2.77 at 3.55μm).

We based the ZBLAN fiber design on the material dispersion by Gan [32] and material loss by FiberLabs Inc., Japan [33]. The particular SIF design considered here was in [37] shown

#203541 - $15.00 USD Received 20 Dec 2013; revised 3 Feb 2014; accepted 3 Feb 2014; published 12 Feb 2014

to be able to generate a 1-4.1μm SC directly from a 1550nm Er laser. The fiber has a core diameter of 5.7μm and Numerical Aperture (NA) of 0.30, which gave the FM a very low but anomalous dispersion with λ_{ZDW}=1.59μm as seen in Fig. 1(b). The low anomalous dispersion allows the generated solitons to rapidly shift to longer wavelengths due to an enhanced Soliton Self-Frequency Shift (SSFS) yielding an efficient MIR SC broadening [37].

For the SC broadening to continue successfully when the ZBLAN SC was coupled into the CHALC fiber it was required that the fiber had; i) a low propagation loss, and ii) anomalous dispersion across most of the transmission window so that the ZBLAN fiber solitons were allowed to further broaden the spectrum. A CHALC MOF having a 20μm core diameter and a grapefruit design has been fabricated by Troles *et al.* with low loss out to 8μm [38] and a similar CHALC MOF was fabricated by Adam *et al.* with low loss out to 8.5μm [39], where in the latter case the long wavelength transmission was set by the As_2Se_3 material loss. Using the grapefruit design we modeled the dispersion for the FM in the 1-9μm range for core diameters of 5 and 20μm based on the As_2Se_3 material dispersion obtained from Amorphous Materials Inc. [34], which is seen in Fig. 1(c). In the large 20μm core the FM was primarily affected by the bulk material dispersion with λ_{ZDW}=6.05μm, which is close to the material λ_{ZDW}=7.55μm. Decreasing the core size enhanced the waveguide contribution to the total fiber dispersion increasing its numerical value thereby shifting the λ_{ZDW} to shorter wavelengths [40]. Decreasing the core diameter down to 5μm shifts the λ_{ZDW} to 3.55μm, which is below the long wavelength transmission edge of the ZBLAN fiber at 4.1μm. This allowed all solitons in the 3.55-4.1μm part of the ZBLAN SC to couple into anomalous dispersion in the CHALC MOF.

Decreasing the size of the fiber core to shift the λ_{ZDW} to shorter wavelengths has the drawback that it increases the fiber losses due to micro-deformations [41-43]. Troles *et al.* measured the loss in a 20μm grapefruit fiber and in a suspended core fiber having a core diameter of 4.5μm at 1.55μm, where they observed an increase of 0.4dB/m larger loss in the smaller core fiber [38]. This is well-known to be due to micro-bending losses [43]. In order to take into account the increased loss due to the micro-deformations in the CHALC MOF having the 5μm core diameter we used the measured loss of a 20μm CHALC grapefruit fiber provided by Perfos [35] and to it add an additional loss of 0.4dB/m at all wavelengths as a worst case scenario, as seen in Fig. 1(c).

Using the dispersion and losses of the ZBLAN and CHALC fibers, as well as the nonlinear material response of the ZBLAN fiber given in [37], and of the As_2Se_3 CHALC composition given by Ung *et al.* [44], the concatenated MIR SC generation was modeled based on the Generalised Nonlinear Schrödinger Equation (GNLSE). We detail on the use of the equation in modeling ZBLAN fiber SC in [37, 45]. The generated MIR SC at the end of each fiber is shown in Fig. 2.

In Fig. 2(a) is shown a single pulse spectrogram of SC at the end of 10m of ZBLAN fiber with spectrum below. We see that the solitons above the λ_{ZDW} at 1.59μm and the Dispersive Waves (DWs) below 1.59μm, nicely follow the total linear group delay $\beta_1 L$ curve (solid black), as is well-known in formation of SC [7]. The time trace in Fig. 2(c) of the ZBLAN fiber SC is only for the 3.5-4.5μm part of the SC and clearly shows the many MIR solitons with peak power around 10kW, which were responsible for the further broadening in the CHALC MOF. An ensemble average of ten pulses is used to evaluate the IR edge (-30 dB level) seen in Fig. 2(e). It shows that SC develops over three meters of the ZBLAN fiber, after which the broadening began to stagnate. The accumulation of the 3-5μm IR power started to stagnate at around 10m, which we took as the optimum length, as here the highest amount of IR power was transferred into the CHALC MOF for further broadening. A longer piece of fiber decreases the IR power due to the fiber losses [37].

Figure 2(b) shows a single pulse spectrogram of the SC at the end of 10cm of the CHALC

#203541 - $15.00 USD Received 20 Dec 2013; revised 3 Feb 2014; accepted 3 Feb 2014; published 12 Feb 2014

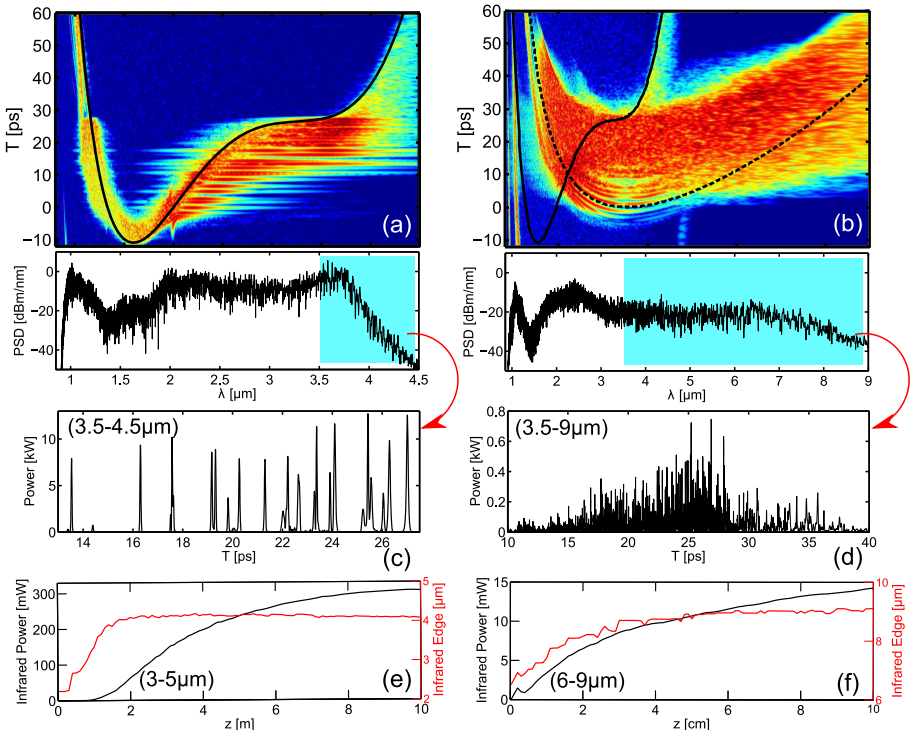

Fig. 2. (a) Spectrogram with the spectrum below of a single pulse SC at the end of 10 m of ZBLAN fiber, and (b) at the end of +10 cm of the 5μm core diameter CHALC MOF. The black solid and dashed lines show the total group delay $\beta_1 L$ for the ZBLAN and CHALC fibers, respectively. (c) Time trace of the 3.5-4.5μm part of the ZBLAN SC, and (d) of the 3.5-9μm part of the CHALC MOF SC. (e) Ten pulse ensemble averaged IR edge (-30dB level) (red) and the accumulated IR power (black) in the 3-5μm range of the ZBLAN SC. (f) The same as (e) for the CHALC MOF SC where the power was evaluated in the 6-9μm range.

MOF having the 5μm core diameter with the spectrum given below. The IR edge of the SC was shifted to 9μm when evaluated at the -30 dB level, which was due to the solitons undergoing SSFS. The short wavelength edge remained at 0.9μm, which was the same wavelength as the ZBLAN fiber SC. The time trace of the 3.5-9μm part of the CHALC MOF SC is seen in Fig. 2(d). Comparing it with the time trace of the ZBLAN SC (see Fig. 2(c)) shows clear soliton fission of the ZBLAN fiber solitons when coupled into the CHALC MOF, as the time trace of the CHALC MOF SC became much denser [7]. The plotted total linear group delay in the single pulse spectrogram evaluated at the end of the CHALC MOF for both the ZBLAN and the CHALC fibers are shown as black solid and dashed lines, respectively. They reveal that the final SC was composed of the SC originating from both fibers, as expected, where the spectral part of the CHALC fiber SC in the 4.5-5μm range on the spectrogram has a clear signature of the long wavelength part of the ZBLAN fiber SC.

In Fig. 2(f) is shown a ten pulse averaged IR edge of the CHALC MOF SC and shows that the SC developed in around 5cm of CHALC MOF due to a combination of the high peak power ZBLAN fiber solitons and the strong nonlinearity of the As_2Se_3 composition. Just as the ZBLAN fiber SC is broadened as the solitons undergo SSFS, the solitons coupling into the anomalous dispersion of the CHALC MOF continued to undergo SSFS and move the IR edge

#203541 - $15.00 USD Received 20 Dec 2013; revised 3 Feb 2014; accepted 3 Feb 2014; published 12 Feb 2014

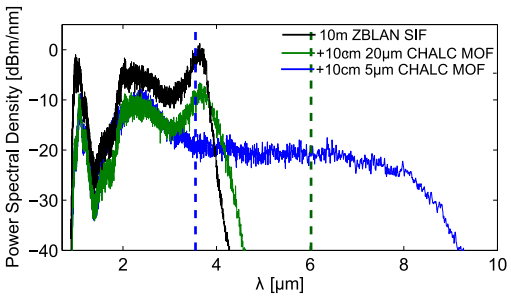

Fig. 3. Comparison between ten pulse averaged SC spectrum of 10m of the ZBLAN fluoride fiber and +10cm of concatenated CHALC MOF having 5μm and 20μm core diameter. The vertical blue and green dashed lines are λ_{ZDW} of the 5 and 20μm CHALC MOFs, respectively.

to the long wavelength transmission edge of the CHALC MOF. The accumulated power in the 6-9μm range shows that around 15mW power could be converted over 10cm of CHALC MOF.

Finally, we compared the influence of the dispersion of the CHALC MOF on the SC generation by comparing the obtained spectrum in the small 5μm and the large 20μm CHALC MOF, as seen in Fig. 3. When transferring the ZBLAN SC into the 20μm CHALC MOF with normal dispersion below λ_{ZDW}=6.02μm (green dashed), the solitons just undergo Self Phase Modulation (SPM) leading to a minor broadening. On the other hand, when transferring the ZBLAN fluoride SC into the 5μm CHALC fiber, the long wavelength part of the SC overlaps with the CHALC anomalous dispersion regime beginning at λ_{ZDW}=3.55μm (blue dashed line) thereby allowing the ZBLAN fiber solitons to continue to undergo SSFS and further push the IR edge to 9μm. Apart from the optimised dispersion, the 5μm core diameter fiber also had a 16 times smaller effective mode area resulting in a much stronger nonlinearity, which additionally enhances the broadening in the 5μm core MOF compared to the 20μm one.

The presented results show that when pumping properly designed concatenated ZBLAN and CHALC fibers with a standard pulsed Tm laser it is possible to obtain an SC spanning from the short wavelength edge of the ZBLAN SC at 0.9μm to the long wavelength edge of the CHALC MOF SC at 9μm. A broadening of more than three octaves has thus been obtained without the need of expensive and intricate pump laser sources.

3. Conclusion

In conclusion, we have demonstrated how a more than three octave broad - 0.9-9μm (-30dB level) - MIR SC could be generated from a standard 2μm Tm mode-locked laser by concatenating (commercially available) ZBLAN step-index fibers with λ_{ZDW} below 2μm with properly designed (commercially available) CHALC MOFs.

The ZBLAN SC extended to 4.1μm, and we showed how a CHALC MOF with λ_{ZDW} sufficiently below 4.1μm was suitable, because it allowed enough of the high peak power solitons in the IR part of the first ZBLAN fiber SC to couple into anomalous dispersion and continue to redshift and broaden the spectrum.

The particular MOF we chose was a 5μm core diameter grapefruit MOF, but the concept applies to any CHALC fiber with a λ_{ZDW} sufficiently below the IR edge of the applied first SC. With the chosen configuration we were able to generate an MIR spectrum with an average power of 15mW above 6μm from the 2W average power 30MHz Tm pump laser. This can be improved upon in several ways. The ZBLAN SC can be improved to have a higher IR power and extend further into the infrared to say 4.75μm, as was recently demonstrated [12]. A tellurite or

#203541 - $15.00 USD Received 20 Dec 2013; revised 3 Feb 2014; accepted 3 Feb 2014; published 12 Feb 2014

indium fluoride (InF_3) [46] fiber with the loss edge at a longer wavelength could be used instead of the ZBLAN fiber. The two approaches each serve to push more power out into the infrared part of the first SC. Given a fixed first SC, the CHALC fiber could be improved to have a lower λ_{ZDW} and longer wavelength loss edge [18, 47]. Thus there is amble room for improvement of this first demonstration of a 0.9-9μm SC, in which we used only commercially available fibers and pump lasers.

Acknowledgments

We thank Kristian Nielsen for fruitful discussion on micro- and macro-bending losses in microstructured fibers. This research has been supported by the European Commission through the Framework Seven (FP7) project MINERVA (317803; www.minerval-project.eu), and the Danish National Advanced Technology Foundation, Grant No. 132-2012-3.

#203541 - $15.00 USD Received 20 Dec 2013; revised 3 Feb 2014; accepted 3 Feb 2014; published 12 Feb 2014